Proposal of fatigue life evaluation method for steel structural details under variable-amplitude stresses

Autor(en): **Mori, Takeshi**

Objekttyp: **Article**

Zeitschrift: **IABSE reports = Rapports AIPC = IVBH Berichte**

Band (Jahr): **76 (1997)**

PDF erstellt am: **23.07.2024**

Persistenter Link: https://doi.org/10.5169/seals-57477

Proposal of Fatigue Life Evaluation Method for Steel Structural Details under Variable-Amplitude Stresses

Takeshi MORI
Professor
Hosei University
Tokyo, Japan

Takeshi Mori, born in 1955, graduated in civil engineering from Tokyo Metropolitan University in 1978, and received his doctor degree from Tokyo Institute of Technology in 1987.

Summary

Fatigue crack propagation analyses for typical steel structural details are performed under various types of variable-amplitude stresses which can approximately express the stress spectrum in various steel structures. On the basis of the analytical results, the relationship between threshold stress range to give the fatigue damage and the degree of fatigue damage is verified. By using this relationship, a new method is proposed to predict the fatigue life under variable-amplitude stresses.

1. Introduction

Fatigue strength or life of the structural details, which is essential in fatigue assessments for the steel structures subjected to repeated action of loads, is usually obtained from fatigue tests under constant-amplitude stresses. However, stresses occurred on the structural details are rarely constant-amplitude but are usually variable-amplitude. This is so, because the load applied to the actual structure is not fixed and their location is also not definite. The fatigue life under such variable-amplitude stresses is generally obtained from the following processes.

(1) The stress range histogram is calculated by applying a stress counting method such as the rain-flow method to the stress variations.
(2) To the stress range histogram and the relationship between stress range and fatigue life ($\Delta\sigma$-N relationship) under constant-amplitude stresses, a linear cumulative damage law is applied, then the fatigue life is obtained.

As the liner cumulative damage law, some methods have been proposed such as Miner's rule, modified Miner's rule, Haibach's procedure and so on, and they are employed in some fatigue design guidelines.

In the cumulative damage law, the fatigue life is basically calculated on the basis of the following equation :

$$D = \Sigma D_i = \Sigma (n_i / N_i) = 1 \qquad (1)$$

in which, n_i is the number of repetitions of $\Delta\sigma_i$ which composes the stress range histogram, N_i is the fatigue life when $\Delta\sigma_i$ are repeatedly applied to the objective detail, as shown in Figure 1. D is the cumulative damage and D_i is the fatigue damage due to $\Delta\sigma_i$. In Miner's rule, N_i is directly computed from the relationship between stress range and a fatigue life obtained from constant-amplitude stress tests, that is, N_i is infinite when $\Delta\sigma_i$ is less than the fatigue limit. However, once the fatigue cracks are initiated under the variable-amplitude stresses, a lower stress component below the fatigue limit becomes effective in causing fatigue damage. The Miner's rule therefore results in giving unsafe estimation. In order to improve this problem, the modified Miner's rule and Haibach's procedure were proposed. In the modified Miner's rule, the N_i according to the

$\Delta\sigma_i$ below the fatigue limit is computed from a straight line extended from the relationship above the fatigue limit, as shown in Figure 1. In this case, it is known that an evaluation becomes too conservative. For that reason, it was proposed that a cut-off limit of stress range was set at below the fatigue limit. Hereafter, this method will be called the modified Miner's rule with the cut-off limit. This method has been employed in "Fatigue Design Recommendations for Steel Structures" by the Japanese Society of Steel Construction (JSSC Recommendations) [1], in which the cut-off limit is set at 46% of the fatigue limits.

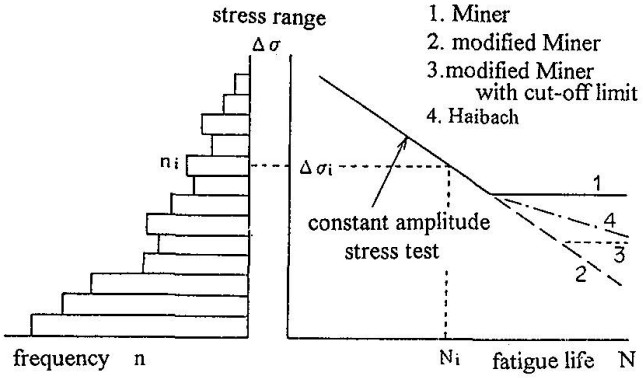

Fig. 1 Linear cumulative damage law

In Haibach's procedure, a slope of $\Delta\sigma$-N relationship below the fatigue limit is more gentle than that above the fatigue limit, as shown in Figure 1. This slope is -1/(2m-1), where -1/m is the slope in a region of stress range being larger than the fatigue limit. This was derived from the following two assumptions. The first was that the threshold stress range ($\Delta\sigma_w$) providing fatigue damage decreases as the cumulative damage (D) increases as shown in Equation (2).

$$\Delta\sigma_w = \Delta\sigma_{wo} (1 - D)^{1/(m-1)} \quad (\Delta\sigma_{wo} : \text{fatigue limit}) \tag{2}$$

Secondly, the cumulative damage (D) is proportional to the cyclic number of every stress range. Reppermund [2] suggested that the later assumption is invalid, and proposed the new method using only the former assumption. Iida and Koh [3] was discussing the value of exponent in Equation (2) on the basis of the fatigue test results on notched specimens of plain steel.

In this study, the $\Delta\sigma_w$-D relationship for typical structural details will be discussed on the basis of fatigue crack propagation analyses under various types of variable-amplitude stresses. A proper parameter for representing the relationship between $\Delta\sigma_w$ and D which can be applied to various structural details will be verified, then a new method will be proposed for predicting the fatigue life under variable-amplitude stresses. Estimation by the proposed method will be compared with estimation by previous methods through the results of the fatigue crack propagation analyses and experimental results by Melhem and Klippstein [4].

2. Fatigue crack propagation analysis

2.1 Analytical models

Objective models consist of three kinds. In the first models, a main plate thickness of a cruciform fillet welded joint shown in Figure 2(a) is varied from 9 to 75mm as indicated in Table 1. An attachment plate thickness is the same as that of the main plate. The width of the joint is three times as large as the plate thickness and weld size is a half of the plate thickness. Weld toe radius and flank angle are assumed to be 0.5mm and 135 degrees. An initial crack is a surface one of semi-elliptical form whose depth is 0.1mm and width is 0.4mm. Its position is assumed to be the center of the plate width. The critical crack depth is supposed to be 80% of the main plate thickness.

In the second models, the weld toe flank angle of the cruciform fillet welded joints shown in Figure 2(a) is varied from 100 to 150 degrees. The thicknesses of both the main and attachment plate are 16mm. The width of the main plate is 110mm, and the weld size is 6mm. The initial and final cracks are the same as those of the first models.

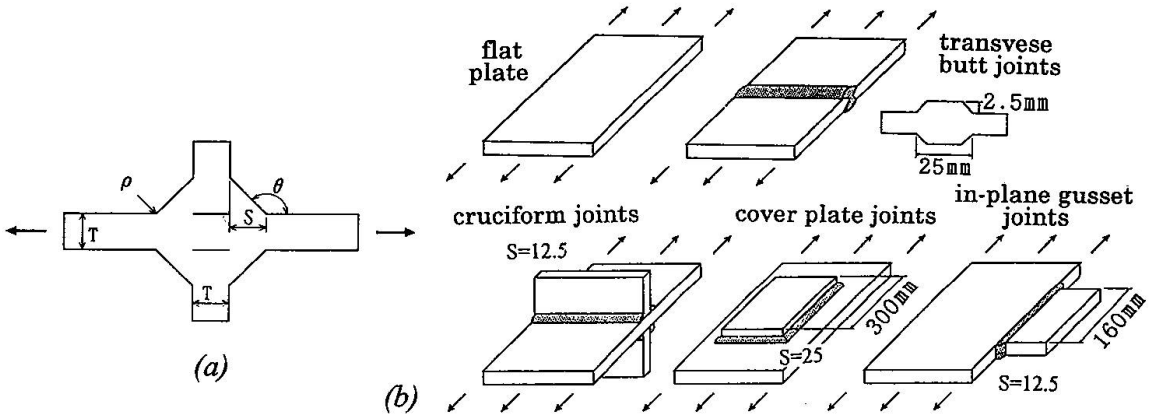

Fig. 2 Analytical models

In the last models, a flat plate, a transverse butt welded joint, a cruciform fillet welded joint, a cover plate welded joint and an in-plane gusset welded joint are taken up. In every joint, its plate thickness is 25mm and its width is 320mm. The flank angle and radius of a weld toe is set at 135 degrees and 0.5mm. The weld size is 12.5mm in the cruciform joint, 20mm in the cover plate joint and 12.5mm in the in-plane gusset joint. For the in-plane gusset joint, the surface initial crack of semi-elliptical form whose depth is 0.1mm and width is 0.4mm is set at the center of the thickness along the weld toe. For other joints, the same initial crack is placed at the center of the width. The critical size of the crack is 80% of the thickness for the cruciform joint and 80% of the width for the other joints.

2.2 Stress range histogram

The fatigue crack propagation analysis will be performed under various stress range histograms which is expressed by the Weibul distribution used in Norwegian standard for mobile offshore structures [5] and is formulated as follows.

$$Q(\Delta\sigma/\Delta\sigma_{max}) = \exp[-(\Delta\sigma/\Delta\sigma_{max})^h \ln(No)] \quad (3)$$

$Q(\Delta\sigma/\Delta\sigma_{max})$	:	cumulative distributed function
h	:	parameter for expressing the shape of the distribution
No	:	total number of stress cycles
$\Delta\sigma_{max}$	:	maximum stress range

The parameters in this distribution are assumed that h is 0.5, 0.7, 1.0, 1.5, 2.0 and No is 10^4, $2x10^4$, $5x10^4$, 10^5, $2x10^5$, $5x10^5$, 10^6, 10^8. That is, 40 types of stress range histograms are employed.

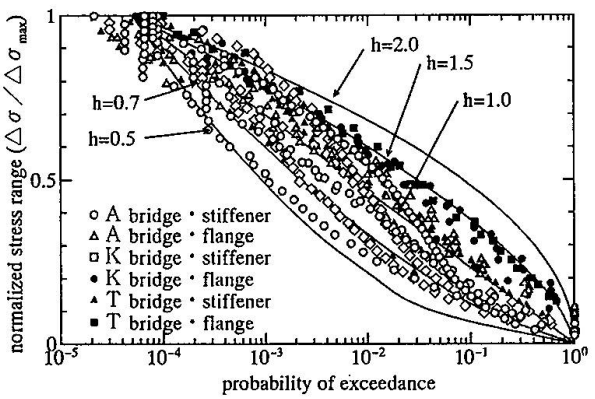

Fig. 3 Cumulative stress range histograms measured in highway bridges

Figure 3 shows the cumulative stress range histograms which were measured on the flange and the stiffener in the actual steel bridges for 24 hours by the Japanese Ministry of Construction [6]. These histograms almost sit between the Weibul distributions of h=0.5 and 2.0. In this figure, 23 histograms are presented and No-values in the 23 histograms range from 8,410 to 80,330. The solid lines are shown for the condition that No is equal to 20,000.

2.3 Analytical procedure

The flow of the fatigue crack propagation analysis used here is shown in Figure 4.

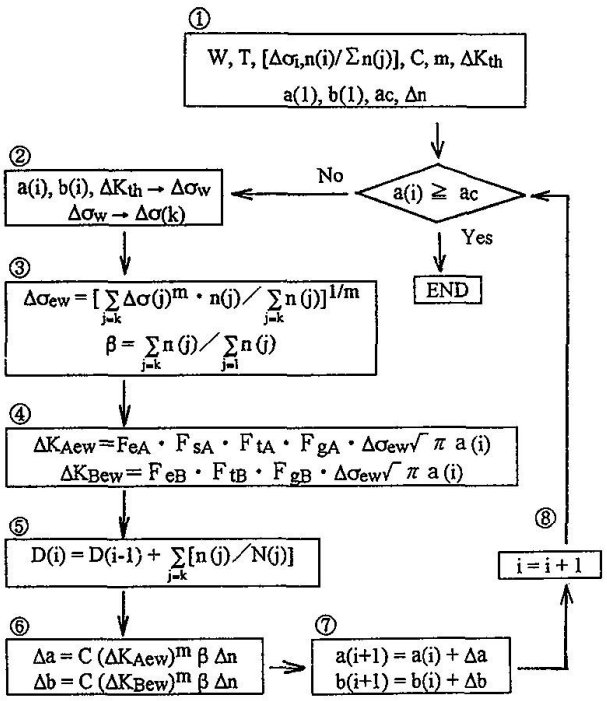

Fig. 4 Process of fatigue crack propagation analysis

① The joint sizes (W, T), the initial crack size [a(1), b(1)], the critical crack size (a_c), the material constants for the fatigue crack propagation rate expression (C, m, ΔK_{th}) and the relative stress range histogram [$\Delta\sigma(j)$, $n(j)/\Sigma n(j)$] are inputted.

② Threshold stress range ($\Delta\sigma_w$) for a given crack is calculated on the basis of the threshold stress intensity factor range (ΔK_{th}).

③ Equivalent stress range ($\Delta\sigma_{ew}$) for the stress components above $\Delta\sigma_w$ is calculated. A ratio (β) of frequency of the stress ranges above $\Delta\sigma_w$ to that of all the stress ranges is also calculated.

④ Equivalent stress intensity factor ranges according to the $\Delta\sigma_{ew}$ and the given crack (ΔK_{Aew}, ΔK_{Bew}) are calculated.

⑤ The cumulative damage (D) is calculated.

⑥ The fatigue crack increments (Δa, Δb) are calculated by using the fatigue crack propagation rate expression.

⑦ The crack after extension is defined.

⑧ Above processes from ② to ⑦ are repeated until the crack is getting large and reaches the final size.

The fatigue crack propagation rate da/dN is expressed as a function of stress intensity factor range (ΔK) by the following equation.

$$\begin{aligned} da/dN &= 5.4\times10^{-12}\,(\Delta K)^3 \quad [\Delta K>\Delta K_{th}] \\ da/dN &= 0 \quad [\Delta K\le\Delta K_{th}] \end{aligned} \tag{4}$$

da/dN : m/cycle,
ΔK : MPa$\sqrt{m}$,
ΔK_{th} = 2MPa$\sqrt{m}$

Equation (4) has been derived from the statistic analysis using many fatigue crack propagation test results on plain steel and welded steel specimen [7]. The value of the threshold stress intensity factor range (ΔK_{th}) was obtained from the test results on the welded specimens in which the fatigue cracks propagated in high tensile residual stress field [8].

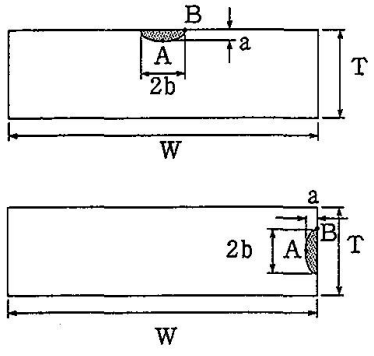

Fig. 5 Definition of a fatigue crack

The stress intensity factor ranges at the deepest point (point A in Figure 5) and the wedge (point B in Figure 5) of the crack are calculated by the following equations :

$$\begin{aligned} \Delta K_A &= F_{eA}\cdot F_{sA}\cdot F_{tA}\cdot F_{gA}\cdot\Delta\sigma\sqrt{\pi a} \\ \Delta K_B &= F_{eB}\cdot F_{tB}\cdot F_{gB}\cdot\Delta\sigma\sqrt{\pi a} \end{aligned} \tag{5}$$

F_{eA}, F_{eB} : correction factor for crack shape
F_{sA} : correction factor for surface crack
F_{tA}, F_{tB} : correction factor for finite thickness and width of plate
F_{gA}, F_{gB} : correction factor for stress gradient

These correction factors could be calculated using the approach given in [9].

The equivalent stress range for the stress range components above the threshold stress range ($\Delta\sigma_{ew}$) can be obtained from the following equation.

$$\Delta\sigma_{ew} = (\Sigma\Delta\sigma_i^3 \cdot n_i / \Sigma n_i)^{1/3} \quad (6)$$

In which, n_i according to $\Delta\sigma_i$ below $\Delta\sigma_w$ is equal to 0.

3. Relationship between threshold stress range and cumulative damage

3.1 Influence of the form of stress range histogram

The relationships between the threshold stress range ($\Delta\sigma_w$) and the cumulative damage (D) are shown in Figure 6(a) for the transverse butt joints and in Figure 6(b) for the cover plate joints, which were obtained from the crack propagation analyses. The ordinates in these figures are the threshold stress range normalized by the fatigue limit ($\Delta\sigma_w/\Delta\sigma_{wo}$). In these figures, analytical results for ten forms of the stress range histograms are indicated, and $\Delta\sigma_w/\Delta\sigma_{wo}$-D relationships are not dependent on the form in both joints. This fact was common in other forms of the stress range histograms and other type of joints.

The results shown in Figures 6(a) and (b) were obtained when the maximum stress range ($\Delta\sigma_{max}$) was set at four times as large as $\Delta\sigma_{wo}$. However, $\Delta\sigma_w/\Delta\sigma_{wo}$-D relationships were not also influenced by the value of $\Delta\sigma_{max}$.

mark	weibul parameters	mark	weibul parameters
○	h=0.5, No=5x10^4	●	h=0.5, No=5x10^5
△	h=0.7, No=10^4	▲	h=0.7, No=10^8
□	h=1.0, No=10^8	■	h=1.0, No=2x10^5
▽	h=1.5, No=2x10^4	▼	h=1.5, No=10^5
◇	h=2.0x10^8	◆	h=2.0, No=5x10^4

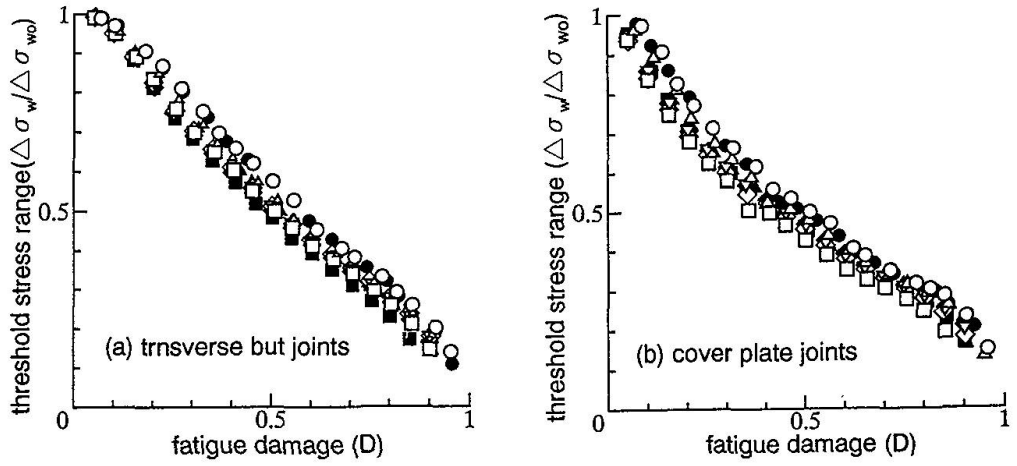

Fig. 6 Influence of stress range histogram on $\Delta\sigma_w$-D relationship

3.2 Influence of plate thickness

For the models in which the plate thickness of the cruciform fillet welded joints is varied from 9 to 75mm, the stress concentration factor obtained from the finite element analyses and fatigue strength at two million stress cycles calculated by the fatigue crack propagation analyses under constant-amplitude stresses are also shown in Table 1. In the finite element analysis, a plane strain element was used, and the minimum element size was set at 0.025mm. These conditions are common to other types of models. As the plate thickness is increasing, the stress concentration is also becomes higher and the fatigue strength becomes lower.

Figure 7 shows the $\Delta\sigma_w/\Delta\sigma_{wo}$-D relationships which were obtained from the crack propagation analyses under variable-amplitude stresses. The form of $\Delta\sigma_w/\Delta\sigma_{wo}$-D relationship becomes concave as the plate is getting thicker, that is, the fatigue strength is decreasing.

model	thick-ness	stress concentration factor	fatigue strength at 2million stress cycles	exponent C
AT	9mm	2.48	178.0MPa	1.23
BT	16mm	2.82	105.0MPa	1.15
CT	25mm	3.25	95.7MPa	1.06
DT	35mm	3.61	89.3MPa	1.00
ET	45mm	3.98	84.8MPa	0.94
FT	75mm	4.61	75.9MPa	0.87

Table 1 Models of varying thickness

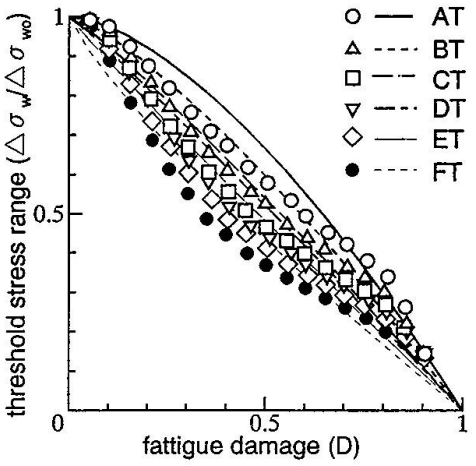

Fig. 7 Influence of thickness on $\Delta\sigma_w$-D relationship

3.3 Influence of flank angle

The stress concentration factor and the fatigue strength at two million stress cycles obtained for the models of varying a flank angle of the weld toe are indicated in Table 2. As the flank angle is getting smaller, the stress concentration factor becomes higher and the fatigue strength becomes lower. It can be seen from Figure 8 that as the fatigue strength becomes lower, the form of the $\Delta\sigma_w/\Delta\sigma_{wo}$-D relationship becomes more concave. This fact is the same as that in the models of varying thickness.

model	flank angle	stress concentration factor	fatigue strength at 2 million stress cycles	exponent C
F150	150ß	2.42	96.6MPa	1.24
F135	135ß	2.76	90.3MPa	1.17
F120	120ß	3.17	84.7MPa	1.11
F100	100ß	3.26	81.4MPa	1.08

Table 2 Models of varying weld toe geometry

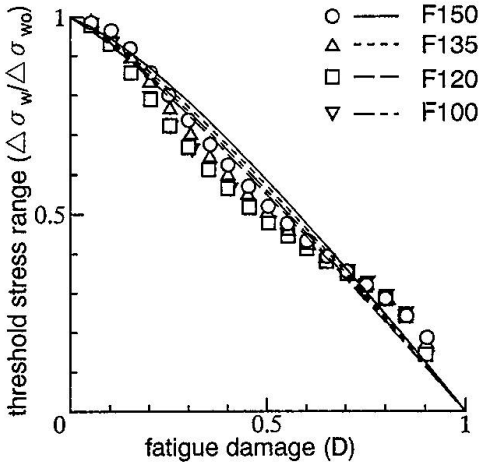

Fig. 8 Influence of flank angle on $\Delta\sigma_w$-D relationship

3.4 Influence of joint type

The stress concentration factor and the fatigue strength at two million stress cycles obtained for each joint indicated in Figure 2(b) are shown in Table 3, and the $\Delta\sigma_w/\Delta\sigma_{wo}$-D relationships for these joints are illustrated in Figure 9. In the same way as the two types of models mentioned above, while the fatigue strength at two million stress cycles becomes lower, the form of the $\Delta\sigma_w/\Delta\sigma_{wo}$-D relationship becomes more concave.

model	stress concentration factor	fatigue strength at 2 million stress cycles	exponent C
flat plate	1.00	178.0MPa	2.06
transverse butt joint	2.32	116.9MPa	1.45
cruciform joint	3.02	86.0MPa	1.12
cover plate joints	3.86	76.3MPa	1.02
in-plane gusset joints	10.95	47.6MPa	0.68

Table 3 Models of varying joint type

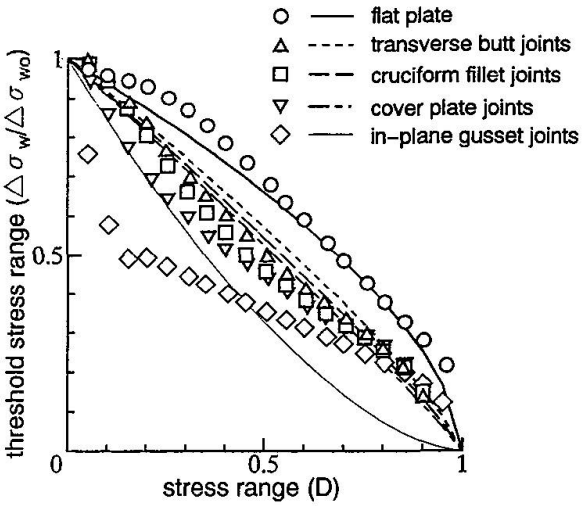

Fig. 9 Influence of joint type on $\Delta\sigma_w$-D relationship

3.5 Expression for the $\Delta\sigma_w/\Delta\sigma_{wo}$-D relationship

The $\Delta\sigma_w$-D relationships shown in Figures 7, 8 and 9 will be expressed by Equation (7) :

$$\Delta\sigma_w = \Delta\sigma_{wo}(1 - D^c) \tag{7}$$

in which, an exponent (c) is a parameter which expresses the form of the $\Delta\sigma_w$-D relationship. When c is equal to unity, the relationship is linear. The form is concave if c is less than unity and convex if c is larger than unity. The value of c for each model is shown on the right hand column of Tables 1, 2 and 3, which was obtained from the least square method. The relationship obtained by the substitution of the c value into equation (7) is also illustrated in Figs.7 to 9. Only a $\Delta\sigma_w$-D relationship for one stress range histogram was shown in Figs.7 to 9, but the value of c was obtained by using the data regarding the relationships in all the stress range histograms (40 types) and 5 to 15 values of $\Delta\sigma_{max}$ for each histogram.

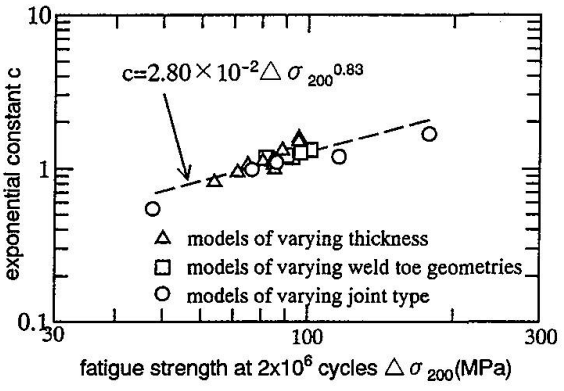

Fig. 10 c-$\Delta\sigma_{200}$ relationship

As mentioned in Sections 3.2 to 3.4, lowering the fatigue strength at two million stress cycles caused the form of the $\Delta\sigma_w$-D relationship to be concave, that is, it effected the value of c to become smaller. The relationship between the values of c and the fatigue strength at two million stress cycles ($\Delta\sigma_{200}$) is shown in Figure 10. This relationship can be expressed by a straight line in both the logarithmic scales. The following expression indicates the c-$\Delta\sigma_{200}$ relationship calculated by the least square method.

$$C = 2.80 \times 10^{-2}\,\Delta\sigma_{200}^{0.83} \tag{8}$$

4. Proposal of fatigue life evaluation method

In this study, the following method is proposed for evaluating the fatigue life under variable-amplitude stresses.

(1) The relationship between stress range ($\Delta\sigma$) and fatigue life (N), the fatigue strength at two million stress cycles ($\Delta\sigma_{200}$) and the fatigue limit ($\Delta\sigma_{wo}$) under constant-amplitude stresses is determined on the basis of the fatigue test results on the objective joints.

(2) By substitution of $\Delta\sigma_{200}$ into equation (8), the value of the exponent c is determined.

(3) By substituting $\Delta\sigma_{w200}$ from step (1) and the value of c from step (2) into Equation (7), $\Delta\sigma_w$-D relationship is determined.

(4) By using the stress range component ($\Delta\sigma_i$) larger than $\Delta\sigma_w$ obtained from equation (7), its relative frequencies(γ_i) and fatigue life (N_i) according to $\Delta\sigma_i$, the cumulative damage is calculated.

$$D = \Sigma(\gamma_i \Delta n / N_i) \quad \text{(if } \Delta\sigma_i \text{ is less than } \Delta\sigma_{wo},\ N_i = \infty)$$

(Δn is a certain number stress cycles for reducing the number of repeating calculation.)

(5) Step (4) is repeated until the value of D reaches unity.

5. Comparison with other methods

5.1 Results of fatigue crack propagation analyses

Figures 11(a) and (b) show the relationship between the equivalent stress range ($\Delta\sigma_e$: is calculated by using all the stress range components) and fatigue life for the transverse butt joint and the cover plate joint, in which the relationship is calculated by the fatigue crack propagation analyses, and estimated by the proposed method and previous methods. In both cases, estimated results by each method are almost the same as those by the analyses in a region where stress range is comparably large. On the other hand, in a region where the stress range is small, Miner's rule results in unsafe estimation and the modified Miner's rule give too conservative evaluation. The modified Miner's rule with the cut-off limit slightly result in conservative estimation. Haibach's procedure and Rempermund's procedure produces good estimation for the cover plate joints, but gives a little conservative evaluation for the transverse butt joints. Comparing with those of the previous methods, the estimated fatigue life by the proposed method could express the results of the fatigue crack propagation analyses well in the whole region.

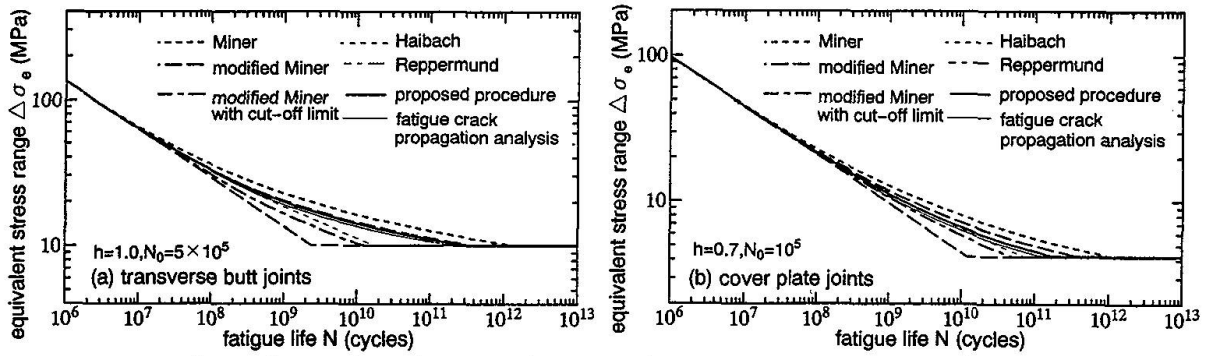

Fig. 11 Relationships between the equivalent stress range and the fatigue life

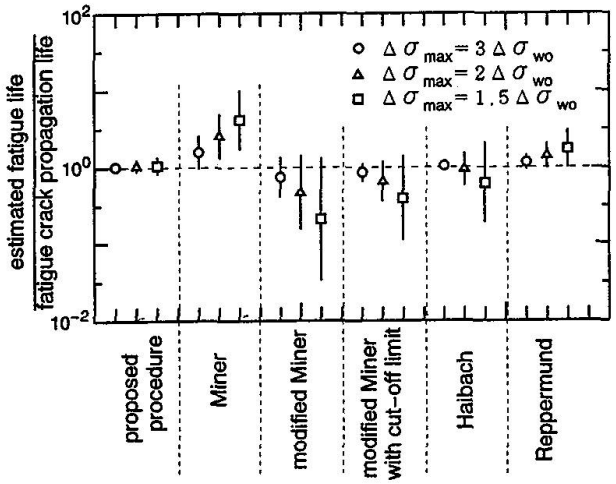

Fig. 12 Comparison of fatigue lives estimated by each method

In order to clarify the differences between the estimated fatigue lives by each method in a region where the stress range is relatively small, the fatigue lives for all the stress range histograms (40 types) and all the models (14 types) are compared for the case that the maximum stress range ($\Delta\sigma_{max}$) is 1.5, 2 or 3 times as large as the fatigue limit ($\Delta\sigma_{wo}$). These results are shown in Figure 12. The ordinate is the fatigue life estimated for each method normalized by that obtained from the fatigue crack propagation analysis. Each mark in the figure shows the average of the normalized fatigue lives and the vertical line indicates the region of the average ± two standard deviations. The normalized fatigue life by the proposed method is almost unity and its deviation is small compared to that of the previous methods.

5.2 Experimental results by Melhem and Kippstein

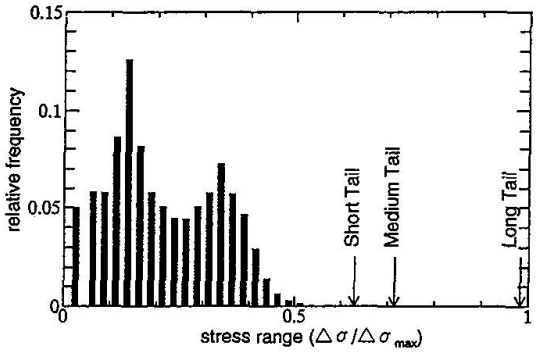

Fig. 13 Stress range histogram used in the tests

Melhem and Kippstein [4] carried out the fatigue tests on the cruciform fillet welded joints (whose thickness is 9.5mm and width is 50.8mm) under constant-amplitude and variable-amplitude stresses. This variable-amplitude stresses simulated the stresses due to the bending moments arising when trucks are passing over the simple supported bridge of 30m span. In this simulation, a distribution of the truck weight was taken into account. The stress range histogram according to the variable-amplitude stresses is shown in Figure 13. This histogram was further divided into three types. Long tail, medium tail and short tail distributions were obtained on the assumption that the truck heavier than 95, 68 and 45 t would not pass, respectively. The materials used for the specimens are A572 steel and A588 steel. The specimens of A572 steel were tested under three kinds of histograms, and those of A588 steel were done under the medium tail distribution only.

Figures 14(a), (b), (c) and (d) show the fatigue test results and the estimated relationships between equivalent stress range ($\Delta\sigma_e$, including all the stress range components) and fatigue life (N) by the proposed method and previous methods. In every series of tests, $\Delta\sigma_e$ -N relationships were obtained up to the region of fatigue lives of eight figures. Until this region, the estimated results by each method are not so different from each other. Observing them in detail, the estimation by Miner's rule, which is considered to give an unsafe estimation, is the closest to the fatigue test results indicated in Figures 14 (a) and (b), and the proposed method is followed. For the test results shown in Figures 14(c) and (d), the proposed method gives the nearest estimation.

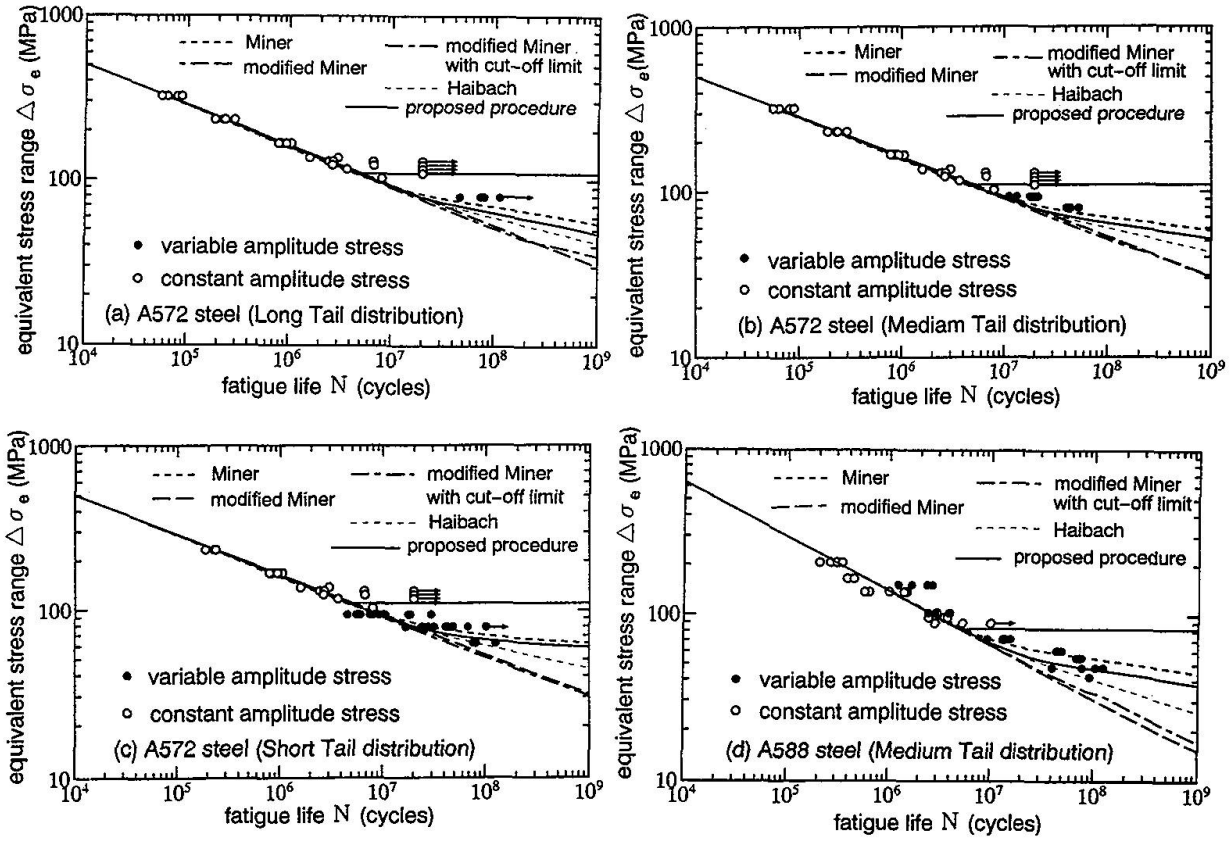

Fig. 14 Comparison of estimated results with the test results

6. Conclusions

(1) The relationship between the threshold stress range and the degree of fatigue damage is significantly influenced by stress distributions in the details. This relationship therefore depends on the type of details, the plate thickness and weld toe geometry.

(2) The relationship for a detail is considerably related to its fatigue strength under constant-amplitude stresses, and can be expressed by the following equation :

$$\Delta\sigma_w = \Delta\sigma_{wo} (1 - D^C)$$

where $c = 2.80 \times 10^{-2} \Delta\sigma_{200}^{0.83}$

$\Delta\sigma_w$: threshold stress range
$\Delta\sigma_{wo}$: fatigue limit under constant-amplitude stress
D : degree of fatigue damage based on a linear cumulative damage concept
$\Delta\sigma_{200}$: fatigue strength at 2 million stress cycles.

(3) The fatigue life evaluation method is proposed by combining the above equation with the linear cumulative damage concept. The validity of the proposed method has been confirmed through the comparisons of fatigue lives estimated by the proposed method to analytical results by crack propagation analysis and to experimental results by Melhem et al.

References

1. JAPANESE SOCIETY OF STEEL CONSTRUCTION. Fatigue Design Recommendations for Steel Structures. JSSC Report No.32, 1995.

2. REPPERMUND, K. Ein Konzept zur Berechnung der Zuver-lassigkeit bei Ermudungsbeanspruchung, Stahlbau, 4/1986, pp.104-112, 1986.

3. IIDA,K. ; KOH,H. Cumulative Fatigue Damage under p-distribution Loads (2nd report), Proc. of The Soc. of Naval Architects of Japan, No.152, pp.372-380, 1982 (in Japanese).

4. MELHEM,H.G. and KLIPPSTEIN, K.H. A study on Variable-amplitude Load Fatigue (work-in-Progress), Research Report No.ST-6, Department of Civil Engineering, University of Pittsburgh, 1990.

5. DET NORSKE VERITAS. Fatigue Strength Analysis for Mobile Offshore Units, Classification Note No.30.2, 1984.

6. CIVIL ENGINEERING RESEARCH INSTITUTE (Japanese Ministry of Construction). A Research on the Techniques about Estimation and Improvement of the Endurance of Exiting Bridges, Report of Civil Engineering Research Institute, No.2420, 1990 (in Japanese).

7 OKUMURA, T., NISHIMURA, T., MIKI, C. AND HASEGAWA, K. : Fatigue Crack Growth in Structural Steel, Proceedings of Japanese Society of Civil Engineers, No.322, pp.175-178, 1982.

8. MIKI,C. ; MORI,T. ; TAJIMA,J. Effect of Stress Ratio and Tensile Residual Stress on near Threshold Fatigue Crack Growth, Proceedings of the Japanese Society of Civil Engineers, No.386, pp.383-392, 1986.

9. MIKI,C. Fatigue Model (Japanese Society of Steel Construction. Reliability Estimation for Civil Structures, Section 5.2), JSSC Report, No.13, pp.89-109, 1989 (in Japanese).